2012

Metal Resistance and Lithoautotrophy in the Extreme Thermoacidophile *Metallosphaera sedula*

Yukari Maezato
University of Nebraska-Lincoln

Tyler Johnson
University of Nebraska-Lincoln

Samuel McCarthy
University of Nebraska-Lincoln

Karl Dana
University of Nebraska-Lincoln

Paul H. Blum
University of Nebraska - Lincoln, pblum1@unl.edu

JB
Journals.ASM.org

Metal Resistance and Lithoautotrophy in the Extreme Thermoacidophile *Metallosphaera sedula*

Yukari Maezato, Tyler Johnson, Samuel McCarthy, Karl Dana, and Paul Blum

Beadle Center for Genetics, School of Biological Sciences, University of Nebraska, Lincoln, Nebraska, USA

Archaea such as *Metallosphaera sedula* are thermophilic lithoautotrophs that occupy unusually acidic and metal-rich environments. These traits are thought to underlie their industrial importance for bioleaching of base and precious metals. In this study, a genetic approach was taken to investigate the specific relationship between metal resistance and lithoautotrophy during biotransformation of the primary copper ore, chalcopyrite ($CuFeS_2$). In this study, a genetic system was developed for *M. sedula* to investigate parameters that limit bioleaching of chalcopyrite. The functional role of the *M. sedula copRTA* operon was demonstrated by cross-species complementation of a copper-sensitive *Sulfolobus solfataricus copR* mutant. Inactivation of the gene encoding the *M. sedula* copper efflux protein, *copA*, using targeted recombination compromised metal resistance and eliminated chalcopyrite bioleaching. In contrast, a spontaneous *M. sedula* mutant (CuR1) with elevated metal resistance transformed chalcopyrite at an accelerated rate without affecting chemoheterotrophic growth. Proteomic analysis of CuR1 identified pleiotropic changes, including altered abundance of transport proteins having AAA-ATPase motifs. Addition of the insoluble carbonate mineral witherite ($BaCO_3$) further stimulated chalcopyrite lithotrophy, indicating that carbon was a limiting factor. Since both mineral types were actively colonized, enhanced metal leaching may arise from the cooperative exchange of energy and carbon between surface-adhered populations. Genetic approaches provide a new means of improving the efficiency of metal bioleaching by enhancing the mechanistic understanding of thermophilic lithoautotrophy.

Nearly 80% of current global copper reserves are comprised of low-quality metal ores (10, 25, 44). Consequently, the need for cost-efficient extraction methods has promoted interest in the use of microbe-based processing. Bioleaching is an established approach for the extraction of base and precious metals from sulfidic ores (30, 34, 35, 43). Bioleaching using thermophilic microbes is of particular importance for certain metals. In the case of copper, elevated temperatures produced naturally in heaps overcome recalcitrant extraction due to surface passivation while chemical reaction rates are accelerated (29, 30). A critical disadvantage of bioleaching is the amount of time required for metal solubilization, often spanning years (22, 38). Therefore, improved metal recovery must include factors that accelerate this process, particularly those inspired by biotechnologic approaches (48).

Thermoacidophilic archaea include taxa that are lithoautotrophic and unusually metal resistant (3, 19). These organisms are native to pyritic or sulfur-rich geothermal habitats and are used to recover base and precious metals from low-quality sulfidic minerals through bioleaching processes (31). In the bioleaching process, both direct and indirect leaching mechanisms have been proposed that convert metals to soluble forms (33, 40). Metal release may occur via metabolic oxidation of the sulfur and iron component of these minerals, thereby releasing other complexed metals, or by direct metal oxidation (41). Recovery rates of copper bioleached from chalcopyrite ranged from 10 to 25% (16), and the recently discovered *Metallosphaera cuprina* was shown to mobilize 10.6% of total copper when grown on chalcopyrite (23). Elucidation of the genome sequence of several biomining organisms (5, 24, 45) along with transcriptomic analyses (4, 20) supports investigations into strategies that underlie lithoautotrophic metabolism.

Among archaea, the distribution of putative copper resistance genes is broad. Many archaeal genomes contain *copA* (P-type ATPase) copper efflux transporters, with the most well-characterized example being found in the hyperthermophilic sulfate reducer *Archaeoglobus fulgidis* (1, 13). Multiple mechanisms of copper resistance also have been identified in *Sulfolobus solfataricus*, including a copper efflux system consisting of *copA* and *copB* (P-type ATPase), *copR* (regulator), and *copT* (metallochaperone) (9, 11, 46, 47). An inorganic polyphosphate symport system identified in the related *Sulfolobus metallicus* has also been predicted to play a critical role in copper resistance (36). Additional predictions concerning the identity of archaeal metallochaperones have been made based on the occurrence of a CxCxC motif and extended variants combined with proximity to metal efflux transporters (12).

Metallosphaera sedula is a lithoautotrophic archaeon originally isolated from a solfataric field in Italy that grows optimally at 70 to 75°C over a pH range of 1 to 4.5 (18). *M. sedula* differs greatly from its relatives, *S. solfataricus* and *S. acidocaldarius*, because the latter organisms are strict chemoheterotrophs with compatible genetic systems (7, 26). In contrast, genetic-based investigations have not yet been used to study lithoautotrophy. Autotrophy in *M. sedula* uses a recently discovered pathway for carbon fixation (6). Stable carbon isotope fractionation has shown that bicarbonate HCO_3^- is used as an inorganic carbon source through the 3-hydroxypropionate/4-hydroxypropionate pathway (6, 32). *M. sedula* is also considerably more resistant to metals than chemoheterotrophic *Sulfolobus* species. For example, cupric ion [Cu(II)] resistance is 20 times greater (18, 46). To gain a

Received 3 August 2012 **Accepted** 5 October 2012
Published ahead of print 12 October 2012
Address correspondence to Paul Blum, pblum1@unl.edu.

doi:10.1128/JB.01413-12

TABLE 1 Plasmids, archaeal strains, and primers

Plasmid or strain	Genotype or characteristics	Source or reference
pBN1078	pJ	This study
pBN1090	pJ::*lacS*$_{S.\ solfataricus}$	This study
pBN1126	pJ::*copRTA*$_{M.\ sedula}$	This study
pBN1260	pUC19::*copA*$_{M.\ sedula}$::*pyrE*	This study
PBL2025	*S. solfataricus* strain 98/2 derivative	39
PBL2090	*S. solfataricus copR*::*lacS* in PBL2069	46
PBL2091	*S. solfataricus* Δ*pyrEF* derivative of PBL2025	This study
PBL2115	*S. solfataricus copR*::*lacS* in PBL2091	This study
PBL2116	*S. solfataricus* pBN1126 in PBL2115	This study
PBL2117	*S. solfataricus* pBN1126 in PBL2091	This study
PBL4000	Wild-type *Metallosphaera sedula*	This study
PBL4001	*M. sedula* spontaneous *pyrE1* derivative of PBL4000	This study
PBL4002	*M. sedula* CuR1 spontaneous copper-resistant derivative of PBL4001	This study
PBL4003	*M. sedula copA*::*pyrE* derivative of PBL4001	This study

better understanding of the interplay between metal resistance, autotrophy, and lithotrophic metabolism, a genetic system was developed for *M. sedula* and used to evaluate parameters governing the efficiency of copper bioleaching.

MATERIALS AND METHODS

Archaeal strains, cultivation, and microscopy. Cell lines used in this study are presented along with their genotypes, origins, and construction details (Table 1). *Metallosphaera sedula* (DSM 5348T) was grown in a basal salts medium (2), adjusted to pH 2.0 at 75°C, in screw-cap flasks with aeration in orbital baths or in glass screw-cap test tubes placed in 150-tube rotary drum agitators mounted in forced-air incubators with external DC motors. Chemoheterotrophic growth used tryptone at 0.05% (wt/vol). A solid complex medium was prepared using basal salts medium mixed with 0.6% (wt/vol) gelrite (Kelco) and supplemented with 0.05% (wt/vol) tryptone. Lithoautotrophic growth used the naturally occurring minerals pyrite (Sargent-Welch) and chalcopyrite (VWR or Alfa Aesar), which had been ground and baked at 200°C for 2 days until sterile. Barium carbonate (witherite) was obtained from Sigma and autoclaved at 120°C for 30 min to sterilize. Planktonic growth was monitored by light adsorption at a wavelength of 540 nm. Epifluorescence microscopy and scanning electron microscopy (SEM) were performed as described previously (5, 37).

Strain construction. Mutations in uracil biosynthesis result in uracil auxotrophy and allowed the use of uracil biosynthetic genes as selectable markers for genetic manipulations. To recover such mutants, pyrimidine analogs, including 5-fluoroorotic acid (5-FOA), were tested on a solid medium and found to severely reduce cell-plating efficiencies. Resistance to 5-FOA in yeast and in the related archaea *Sulfolobus acidocaldarius* (17) and *Sulfolobus solfataricus* (28) has been shown to occur in pyrimidine biosynthetic genes, notably orotidine pyrophosphorylase (*pyrE*) and orotidine decarboxylase (*pyrF*). Spontaneous mutation frequencies for *M. sedula* to 5-FOA resistance were evaluated on solid media containing the analog with and without addition of uracil, and 5-FOA resistance was measured at a frequency of 1/10^6 cells plated. The *pyEF* genes of one purified 5-FOA-resistant isolate that had been confirmed as a uracil auxotroph were sequenced, and the *pyrE* gene was mutated. *M. sedula* transformation was performed as described for *S. solfataricus* (26, 42). Genetic selections for chromosomal recombination were developed using the *pyrE*

TABLE 2 Primers

Primer name	Sequence
Mse490F-SphI	5′ AGCTGCATGCAAGGGAAAGATGTACTACTT CTGC 3′
Mse490R-SphI	5′ AGCTGCATGCATGAATTCTTTGAGATACAC GTCG 3′
MpyrEF-NgoMIV	5′ AGCTGCCGGCCAAGGCTTGGCCTAAACCCGC 3′
MpyrER-NgoMIV	5′ AGCTGCCGGCACAAGTTCCTTAACTTTCTCC 3′
Mse490RTF	5′ CCAGTCAGTGAAGGCCACAAAGGC 3′
Mse490NSTR	5′ TATCGGTATCCTCACGGCCTCTGC 3′

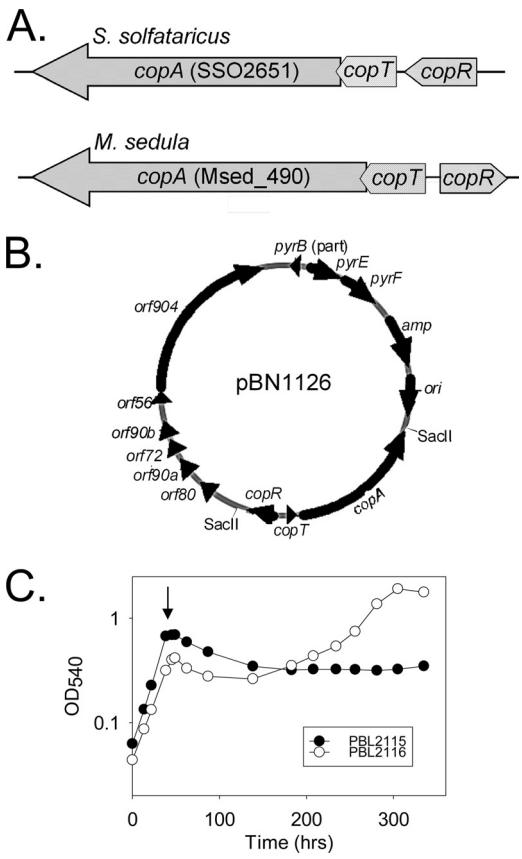

FIG 1 *M. sedula copRTA* analysis by heterologous complementation. (A) *copRTA* locus. (B) pJlacS carrying *M. sedula copRTA*. (C) Copper resistance of pJlacS *M. sedula copRTA* in the *S. solfataricus copR* mutant. Strains were the *S. solfataricus copR* mutant strain (PBL2115; closed circles) and the *S. solfataricus copR* mutant complemented with pJlacS *M. sedula copRTA* (PBL2116; open circles). Cultures were treated (arrow) with 0.75 mM Cu(II) (final concentration).

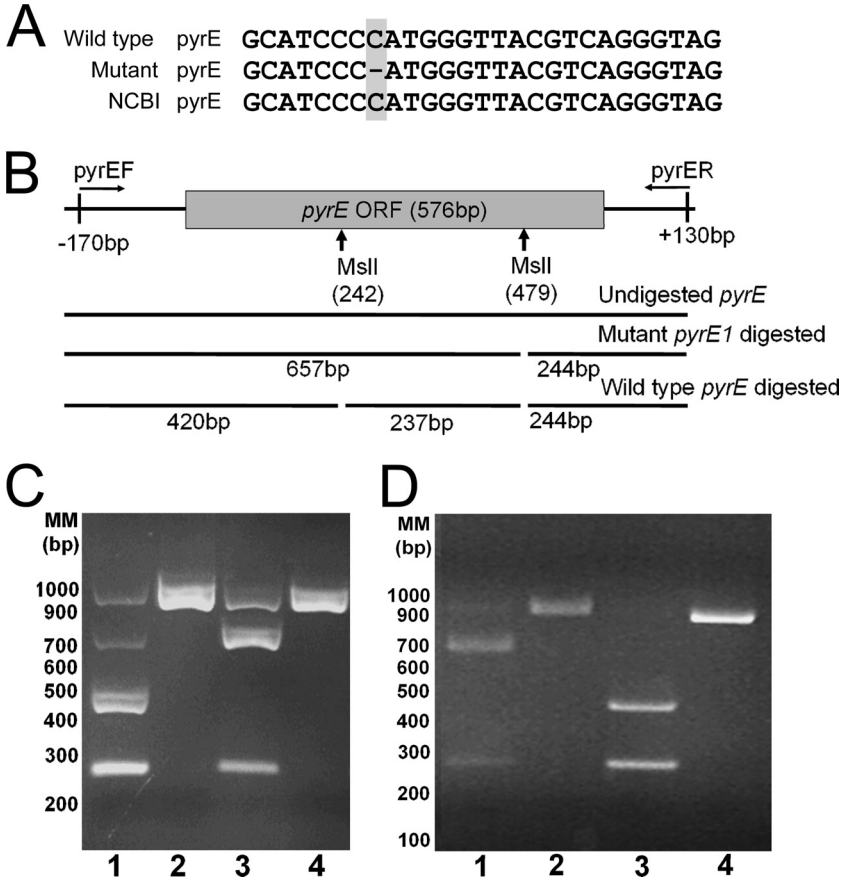

FIG 2 Homologous recombination in *M. sedula*. (A) *pyrE1* mutant sequence compared to the wild-type and NCBI-deposited *pyrE* sequences. (B) Schematic of restriction fragments of the *pyrE1* amplicon. (C) Restriction analysis of the *pyrE1* mutant. Lane 1, wild-type *pyrE* PCR amplicon digested with MslI. Lane 2, wild-type *pyrE* amplicon not digested with MslI. Lane 3, *pyrE1* amplicon digested with MslI. Lane 4, undigested *pyrE1* amplicon. (D) Restriction analysis of *pyrE1* recombinants. Lane 1, *pyrE*1 (PBL4001) amplicon digested with MslI. Lane 2, *pyrE1* undigested amplicon. Lane 3, homologous recombinant *pyrE* amplicon digested with MslI. Lane 4, homologous recombinant undigested *pyrE* amplicon. MM, molecular marker.

gene. PCR amplicons of *pyrE* and the negative-control *pyrF* were transformed by electroporation into the *pyrE1 M. sedula* mutant (Table 2). Transformed cells were grown in dilute tryptone medium lacking uracil, thereby allowing selection for prototrophs. Only *pyrE* mutant cells, transformed with the *pyrE* gene, grew normally in the absence of uracil supplementation. Individual transformed cells were isolated and genotyped by colony PCR combined with MsII restriction analysis of the *pyrE* PCR amplicon. The *copA* knockout strain was constructed by successive single crossovers using a plasmid-encoded disruption construct (pBN1260). First, the *copA* open reading frame (ORF) was amplified using primers Mse490F-SphI and Mse490R-SphI and then was cloned into pUC19 at the SphI site. *M. sedula pyrE* then was cloned into pUC19::*copA* (PB1260) at an NgoMIV site, resulting in plasmid pBN1260, which was then transformed into strain PBL4001 with selection for uracil prototrophy. For complementation studies in *S. solfataricus*, the *M. sedula copRTA* operon was cloned into plasmid pBN1078 at the SacII site to make plasmid pBN1126. The *copR*::*lacS* mutation in *S. solfataricus* strain PBL2090 (46) was transferred into strain PBL2091 (termed the Δ*pyrEF* strain) by the allele transfer method (26), and the new strain was used as the parental strain for the transformation of the *M. sedula copRTA* operon located on plasmid pBN1126. A spontaneous copper-resistant strain (CuR1) was isolated by repeated passage of *M. sedula* in media supplemented with increasing concentrations of $CuSO_4$. Passage involved one cycle with 100 mM $CuSO_4$ supplementation and then three cycles with 200 mM $CuSO_4$ supplementation. Cells were transferred in mid-exponential growth phase. The CuR1 isolate was purified by single-colony isolation followed by retesting metal resistance relative to the wild-type (WT) strain.

qRT-PCR. Quantitative reverse transcription-PCR (qRT-PCR) using SYBR-I green and a real-time PCR instrument (Eppendorf Mastercycler) as described previously (27). RNA was extracted as described previously (8) and treated to remove DNA by addition of 1 U of DNase I (Fermentas) per μg of total RNA at room temperature for 15 min and then neutralized with 2 μl of 25 mM EDTA and incubated at 70°C for 10 min. cDNA synthesis used 20 pmol of PCR antisense primer, 20 mM deoxynucleoside triphosphate (dNTP) mix (Invitrogen), and 200 U of Moloney-murine leukemia virus RT (Fermentas) for 60 min at 37°C. Synthesized cDNA was subjected to standard PCR and analyzed using 2% (wt/vol) Tris-borate-EDTA agarose gels. Primers used for qRT-PCR were Mse490RTF and Mse490NSTR.

Proteomics. Cell suspensions were prepared using intermittent sonication and then analyzed by two-dimensional (2D) SDS-PAGE, and protein identities were determined by tandem mass spectrometry (MS/MS) electrospray analysis using material excised from SDS-polyacrylamide gels (15, 49). Gel slices were infused with trypsin to digest the protein, and the resulting peptides were recovered, separated by capillary electrophoresis prior to MS/MS analysis, and then identified by local BLAST against the *M. sedula* proteome. Fold changes in spot intensity were determined using Phoretix 2D Evolution (Nonlinear Dynamics).

ICP-MS. To determine the extracellular concentrations of copper, culture samples were clarified by centrifugation. Samples of the resulting

supernatants were analyzed by inductively coupled plasma-MS (ICP-MS) using an Agilent ICP-MS 7500cx. A certified copper reference standard was used for sample normalization. All values are averages from triplicate samples.

RESULTS

Functional identity of *M. sedula copRTA*. *Metallosphaera sedula* is unusually resistant to several metals, including copper (18). Genomic features responsible for this trait include two putative copper-translocating ATP-dependent exporters (*copA* and *copB*). A similar situation occurs in the related species *Sulfolobus solfataricus*, though here only *copA* has been shown to be copper inducible (11, 46) and the *copR* transcription factor is transcribed in the opposite direction relative to the situation in *M. sedula* (Fig. 1A). It has been shown previously that the *S. solfataricus copR* mutant can be complemented using the *S. solfataricus copR* gene (46). To verify the functional role and expression of the *M. sedula copRTA* locus, the region was expressed in an *S. solfataricus* mutant lacking copper resistance due to a gene disruption of the *copR* transcription factor gene (46). *M. sedula copRTA* was cloned into *S. solfataricus* plasmid pJ (pBN1078), a derivative of pJLacS (7) lacking *thsAp*::*lacS*. The resulting plasmid (pBN1126) (Fig. 1B) was then transferred into the *S. solfataricus copR* mutant by transformation followed by selection for uracil prototrophy and the isolation of a clonal population on a solid medium. The copper resistance of the *S. solfataricus* plasmid transformant (strain PBL2116) was compared to that of the parental strain (PBL2115) in liquid culture under chemoheterotrophic conditions (Fig. 1C). In response to a 0.75 mM cupric ion [Cu(II)] challenge, a concentration shown previously to induce *S. solfataricus cop* expression (46), heterologous expression of the *M. sedula copRTA* locus in the *S. solfataricus copR* mutant complemented copper sensitivity in an inducible fashion. After induction, the complemented strain gained the ability to growth at 10 mM Cu(II), a concentration nearly twice the level observed for growth of wild-type *S. solfataricus* (46). This finding verifies the functional identity of the *M. sedula copRTA* locus and demonstrates that gene expression signals for transcription and translation are recognized between these organisms.

Role of the *copA* gene in copper resistance of *M. sedula*. While the *M. sedula copRTA* locus conferred copper resistance when expressed in *S. solfataricus*, the level produced was more than 8-fold less than the resistance level of wild-type *M. sedula* (76 mM). This suggested that there are additional factors controlling metal resistance that are native to *M. sedula*, such as *copB* (9, 47) and *ppx* (36). To better understand the importance of *copA*, it was necessary to develop a genetic system in *M. sedula*, and this was pursued in part because cross-species gene expression was successful.

Mutations in pyrimidine biosynthesis result in uracil auxotrophy and allow the use of pyrimidine biosynthetic genes as selectable markers for genetic manipulations. Spontaneous mutations mapping to the *M. sedula pyrE* gene were recovered by following the procedures established for other thermoacidophilic archaea (14, 21). One isolate, termed PBL4001, had a −1 deletion mutation in *pyrE* at nucleotide (nt) 243 relative to the start codon that was called *pyrE1* (Fig. 2A). This mutation shifted the reading frame and resulted in a premature stop codon (TAG) at nt 260, producing a C-terminal truncation and shortening the normal protein from 191 to 86 residues. This mutation also resulted in the loss of one of two restriction sites in *pyrE* for MslI (Fig. 2B and C). Complementation of the *pyrE1* mutation used plasmid pJlacS (pBN1090) that carried the *S. solfataricus pyrEF* genes (7). Recovery of pBN1090 transformants of the *M. sedula pyrE1* mutant (PBL4001) resulted from selection for uracil prototrophy, while the continued presence of the plasmid was determined by the expression of the *S. solfataricus lacS* gene, as indicated by hydrolysis of 5-bromo-4-chloro-3-indolyl-β-D-galactopyranoside (X-Gal) applied topically to colonies and subsequent formation of a blue color. Having verified that *pyrE1* was responsible for the uracil auxotrophic phenotype, repair of this mutation by chromosomal homologous recombination was monitored by changes in *pyrE*-linked restriction polymorphisms. Purified putative recombinants were characterized by PCR amplification of *pyrE* followed by restriction analysis (Fig. 2D) to distinguish between mutant and wild-type *pyrE* alleles. MslI restriction of the wild-type *pyrE* amplicon produced three fragments of 420, 237, and 244 nt that comigrate, while restriction of the *pyrE1* mutant amplicon produced two fragments of 657 and 244 nt. Incompletely digested amplicons are also evident in some lanes as faint large bands. Colony PCR combined with MslI restriction was used as a screen to identify *pyrE* recombinants. *pyrE* recombinants exhibited a

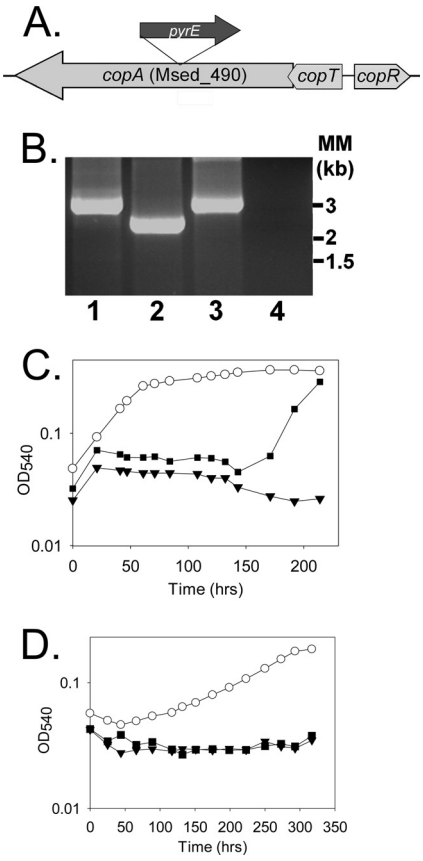

FIG 3 Construction and growth of the *M. sedula copA* mutant and the supranormal copper-resistant isolate CuR1. (A) Schematic of the *copA* disruption construct. (B) PCR genotyping of the *copA* mutant. Lane 1, recombinant *copA* allele. Lane 2, wild-type *copA* allele. Lane 3, *copA*::*pyrE* plasmid. Lane 4, no DNA. (C) Heterotrophic growth at 75 mM Cu(II). OD_{540}, optical density at 540 nm. (D) Heterotrophic growth at 200 mM Cu(II). Shown are CuR1 (open circles), the wild type (closed squares), and the *copA* mutant (inverted closed triangles).

TABLE 3 qRT-PCR analysis

Strain	C_T[a]	Msed_0951 (*tbp*) C_T	ΔC_T[b]	$\Delta\Delta C_T$	$2^{-\Delta\Delta CT}$	Fold change[c]
WT *copA*	10.08	17.28	−7.20	0.92	0.53	1.88
CuR1 *copA*	10.18	18.30	−8.12	0	1	
WT *copB*	16.32	18.22	−1.90	2.08	0.24	4.17
CuR1 *copB*	15.33	19.31	−3.98	0	1	
WT *ppx*	13.46	17.28	−3.82	0.31	0.81	1.23
CuR1 *ppx*	14.17	18.30	−4.13	0	1	

[a] C_T, threshold cycle.
[b] Values were normalized to those of *tbp*.
[c] Fold change comparing the WT to CuR1.

wild-type *pyrE* restriction pattern, as indicated by restoration of the second MslI restriction site. Confirmation of homologous recombination at *pyrE* provided the basis for targeted inactivation of other *M. sedula* genes. The *M. sedula copA* gene (Msed_0490) was then disrupted by insertion of the *M. sedula* wild-type *pyrE* gene following transformation using a circular nonreplicating (suicide) construct (Fig. 3A). The resulting purified isolate was then genotyped by restriction analysis and DNA sequencing of the *copA* locus (Fig. 3B). The level of copper resistance (MIC) of the *copA* mutant was tested under heterotrophic growth conditions relative to the wild-type strain and was found to have been reduced from 76 to 40 mM Cu(II). While this demonstrated a larger role for *copA* as a mediator of copper resistance in *M. sedula* than in *S. solfataricus*, the residual metal resistance of the *copA* mutant remained much greater than that of wild-type *S. solfataricus,* indicating that there are additional factors controlling this trait in *M. sedula*.

Supranormal copper resistance in *M. sedula*. To examine how extreme metal resistance might influence copper leaching, a cell line with greater-than-normal levels of copper resistance was studied. An *M. sedula* strain with increased copper resistance, CuR1, was recovered after repeated subculturing using gradual increases in added Cu(II). After 150 h, inducible resistance to 76 mM Cu(II) challenge was evident for the wild type but not the *copA* mutant (Fig. 3C). Induction of copper resistance was further supported by the observation that adapted cells subcultured into fresh copper-containing medium exhibited no lag. In contrast, the CuR1 strain was constitutively resistant to this amount of copper and exhibited no lag. When the copper challenge was increased to 200 mM Cu(II), the CuR1 mutant exhibited inducible copper resistance while both the wild type and *copA* mutant failed to grow (Fig. 3D). Unexpectedly, CuR1 also exhibited elevated resistance to Cd(II) with a MIC of 10 mM, which was 6 times higher than that of the wild-type strain. DNA sequencing of the primary loci implicated in copper resistance, including *copA*, *copB*, and *ppx*, indicated there were no sequence alterations in any of these ORFs or within 150 nt of flanking DNA. In addition, qRT-PCR analysis of *copA* and *ppx* mRNA normalized to that of a gene encoding the TATA binding protein, *tbp* (Msed_0951), indicated there was less than a 2-fold difference between CuR1 and the wild-type strain; however, *copB* mRNA levels were increased by 4-fold (Table 3). The *S. solfataricus* CopB catalytic domain has been characterized *in vitro* (9), and although its expression *in vivo* is only modestly responsive to copper (46), it does contribute to copper resistance (48), therefore increased expression of *M. sedula copB* in CuR1 may increase copper resistance. To examine the CuR1 strain in additional detail, proteomic analysis by 2D SDS-PAGE was conducted using the CuR1, wild-type, and *copA* mutant strains (Fig. 4). Changes in the abundance of several proteins were evident, and their identities were determined by MS/MS (Table 4). Among the affected proteins were two containing AAA ATPase domains, including Msed_2179 and Msed_2237, which are notable because they could be involved in metal import or efflux. In addition, CopA was identified by proteomic analysis and was absent from the *copA* mutant, thereby verifying the genotype of this strain (Fig. 4). Alterations in metal importer abundance could contribute to the cross-resistance of CuR1 to copper and cadmium.

Role of copper resistance during lithoautotrophy. The importance of copper resistance during lithoautotrophy was examined using chalcopyrite as the energy source and the wild-type, *copA*, and CuR1 strains. Growth and retention of viability was examined after incubation in a chalcopyrite suspension relative to that in a tryptone medium for 14 days. No carbon source was added to the suspension medium. All three strains exhibited equivalent fitness in the tryptone medium, having cell densities between 10^7 and 10^8 after the incubation period (Fig. 5). However, while there was little apparent growth in the chalcopyrite suspension, the wild-type and CuR1 strains retained viability. In contrast, the *copA* mutant was unable to retain viability in the chalco-

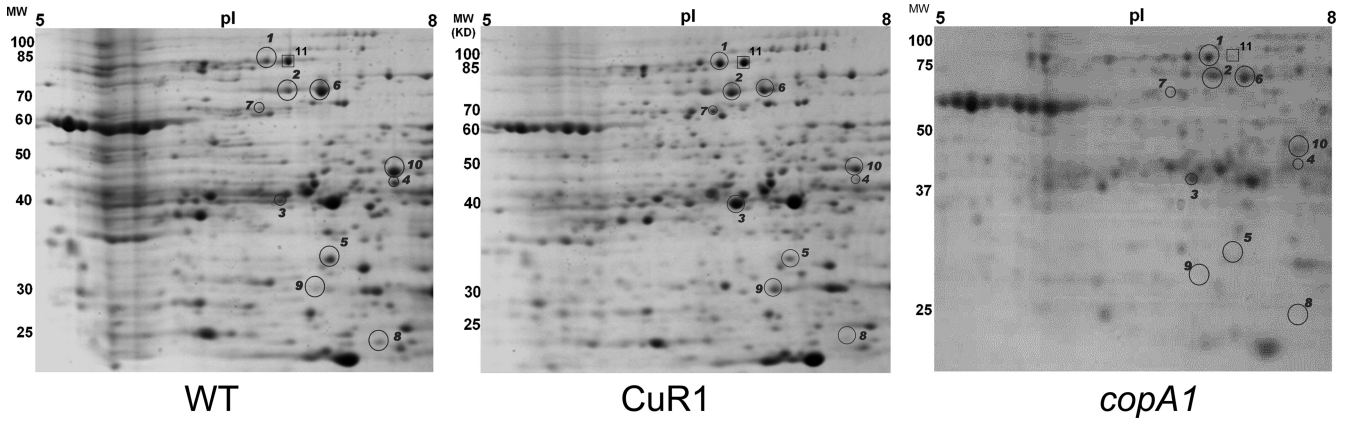

FIG 4 Proteomic analysis of *M. sedula* strains. Two-dimensional SDS-PAGE analysis of *M. sedula* whole-cell extracts. Circles indicate proteins whose abundance varied in the mutants relative to the wild type. Protein identities are shown in Table 4. MW, molecular weight (in thousands).

TABLE 4 Tandem MS identification

Spot	ORF[a] (% coverage)	Abundance[b]
1	Msed_0297 carbon monoxide dehydrogenase (acceptor) (39)	+1.7
2	Msed_2237 AAA family ATPase, CDC48 subfamily (44)	+2.4
3	Msed_2074 Glu/Leu/Phe/Val dehydrogenase, C terminal (77)	+6.5
4	Msed_0534 phosphoribosylglycinamide formyltransferase 2	−4.09
5	Msed_1927 ketol acid reductoisomerase (45)	−3.3
6	Msed_2237 AAA family ATPase, CDC48 subfamily (46)	−2.2
7	Msed_0525 pyruvate flavodoxin/ferredoxin oxidoreductase (34)	+2.6
8	Msed_2179 conserved secretion-like protein (24)	−5.1
9	Msed_0455 lactate/malate dehydrogenase (53)	+4.0
10	Msed_0455 lactate/malate dehydrogenase (18)	−2.0
11	Msed_0490 CopA, copper-translocating P-type ATPase	0.0

[a] MS/MS identification was based on multiple peptide matches for each protein, and the values for total coverage are indicated by percentages in parentheses.
[b] Change in abundance comparing levels observed in *M. sedula* strain CuR1 to those in wild-type *M. sedula* normalized to the CopA strain within each sample.

pyrite suspension, indicating that a functioning copper pump was essential under these conditions.

One reason for the lack of growth of the wild type and CuR1 strain in the chalcopyrite suspension could be the lack of a carbon source. Therefore, addition of the carbonate mineral witherite (barium carbonate) was tested as a possible and more convenient carbon source than those previously described. Unlike magnesium or calcium carbonate, barium carbonate, with a dissociation constant (K_d) of 2.58×10^{-9}, is insoluble in hot acid. *M. sedula* cultured in the presence of witherite colonized the mineral surface, as indicated by epifluorescence microscopy of 4′,6-diamidino-2-phenylindole (DAPI)-stained samples (Fig. 6A). Surface colonization and the formation of adherent cells was also evident by SEM when cells were cultured with the addition of both chalcopyrite and witherite (Fig. 6B). The role of metal resistance and carbon supplementation on copper leaching was examined next using the three strains cultivated with chalcopyrite as the energy source and either with or without witherite addition. Lithotrophic-dependent release of copper was monitored by ICP-MS of clarified culture supernatants (Fig. 7). After a 30-day incubation period, it was apparent that both the allelic state of *copA* and carbon supplementation strongly influenced the lithotrophic metabolism of chalcopyrite. Without carbonate addition, the CuR1 strain released 3.3 times more copper than either of the other two strains. However, with carbonate addition, copper release was greatly stimulated in both the CuR1 and wild-type strains, resulting in the mobilization of 41.5% of total copper from chalcopyrite, reaching 0.4 g/liter (6.3 mM). In contrast, release of copper by the *copA* mutant was negligible regardless of carbonate addition and approximated the values observed with uninoculated controls.

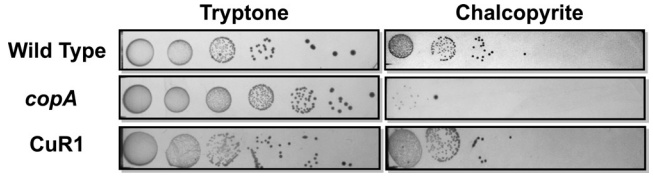

FIG 5 Viability of *M. sedula* strains. Strains were cultured in the presence of 0.2% (wt/vol) chalcopyrite for 14 days. Serial dilutions of culture samples (up to 10^6-fold) were applied to complex medium plates and incubated for 7 days.

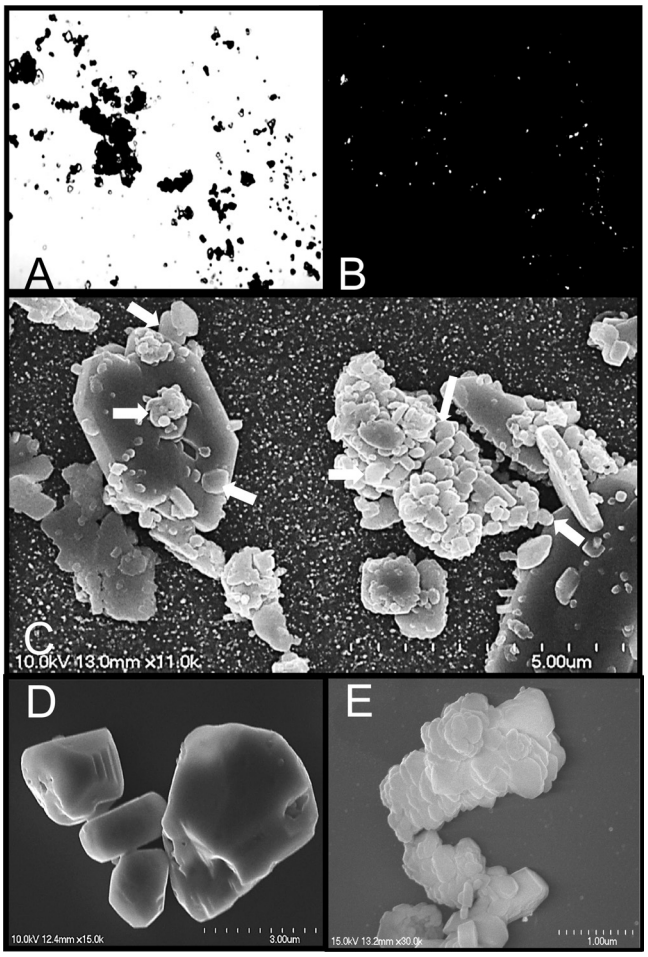

FIG 6 Growth of *M. sedula* on witherite and chalcopyrite. (A) Bright-field microscopy (30× magnification) of *M. sedula* grown with $BaCO_3$. (B) Epifluorescence microscopy of DAPI-stained sample shown in panel A. (C) Scanning electron microscopy of *M. sedula* on crystal surfaces. Witherite ($BaCO_3$) is on the left and chalcopyrite ($CuFeS_2$) is on the right. White arrows indicate cells. (D) Sterile witherite. (E) Sterile chalcopyrite.

DISCUSSION

The results presented here demonstrate a direct relationship between the level of copper resistance and the rate of bioleaching of chalcopyrite during lithoautotrophic cultivation of *Metallosphaera sedula*. Bioleaching requires the oxidation of iron and/or sulfur and therefore provides an indirect measure of lithotrophic metabolism. Thus, the level of copper resistance influences both lithotrophy and bioleaching of copper. The use of modified cell lines specifically altered in genes associated with copper resistance provided direct evidence that metal resistance influences these processes. The interdependence of these traits is of particular relevance to copper but may by relevant to the recovery of other

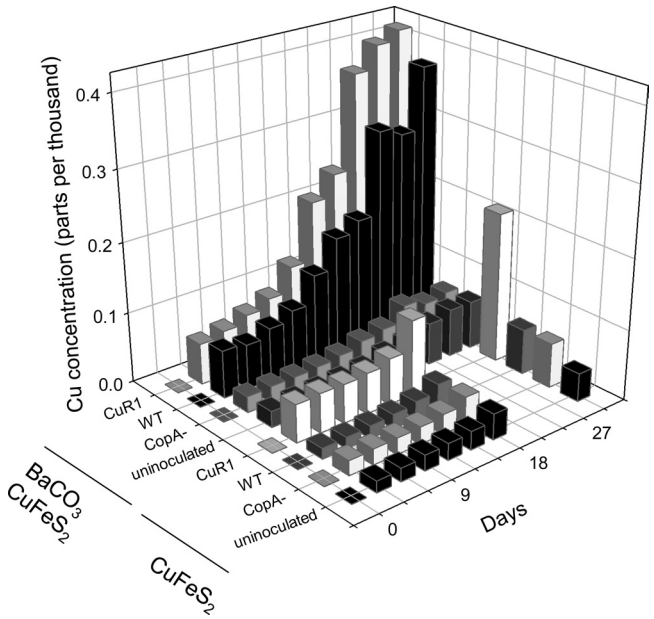

FIG 7 ICP-MS time series analysis of copper leaching. Culture supernatants were collected and sterilized prior to ICP-MS analysis using an Agilent ICP-MS 7500cx calibrated to a certified mercury standard.

metals where metal toxicity presents a challenge to lithotrophic metabolism.

During lithotrophy, copper is released by iron and sulfur oxidation, becoming available to interact with adherent *M. sedula* cells. The importance of copper resistance most likely stems from the ability of cells to exclude or expel excessive intracellular copper ions. In this study, resistance was dependent on copper translocation as the *copA* mutant lost more than half of wild-type levels of copper resistance along with the ability to retain viability during cultivation on chalcopyrite. Additional support for the importance of this relationship was apparent from the behavior of a high-level copper-resistant strain that conducted faster copper leaching than the wild-type strain. This indicates that wild-type levels of copper resistance can be supplemented to overcome excessive metal toxicity.

When assessed by heterologous expression in *S. solfataricus*, the *M. sedula copRTA* genes conferred greater than wild-type levels of metal resistance. This result could arise by several mechanisms. Although the pJ plasmid is a low-copy-number vector (7), it could provide higher-than-normal levels of CopA through increased gene dosage, resulting in higher rates of metal export. Alternatively, the *M. sedula copR* gene could complement the disrupted *S. solfataricus copR* gene and mediate elevated *copTA* transcription above normal levels of expression. While not mutually exclusive, these two mechanisms could be resolved by heterologous expression of either gene alone. Continued resistance of the *M. sedula copA* mutant that exceeded that of wild-type *S. solfataricus* suggests the continued action of other mechanisms for copper resistance. These could include *copB,* as its expression was elevated in the CuR1 strain. However, other components involved in high-level metal resistance of *M. sedula* may remain. One likely mechanism is reduced metal uptake. Simultaneous resistance to copper and cadmium observed in the CuR1 strain could result from reduced rates of metal uptake in addition to elevated expression of *copB*.

While metal resistance was shown to be an important characteristic associated with lithotrophy, provision of additional carbon obscured this difference. The use of insoluble carbonates as an autotrophic nutrient for extremely thermoacidophilic microbes has not been described previously; however, the simultaneous development of witherite and chalcopyrite biofilms suggests adherent cells interact by exchanging leached nutrients. Circulation of soluble bicarbonate (witherite) and iron (chalcopyrite) may provide the carbon and energy required for biofilm expansion. Further developments in the *M. sedula* genetic system will help to expand information on lithoautotrophy and other traits of importance in bioleaching for metal recovery.

ACKNOWLEDGMENTS

This study was supported by funds from the DOD (HDTRA1-09-0030) and NIH (NIGMS 1R01GM090209).

REFERENCES

1. **Agarwal S, et al.** 2010. Structure and interactions of the C-terminal metal binding domain of *Archaeoglobus fulgidus* CopA. Proteins **78**:2450–2458.
2. **Allen MB.** 1959. Studies with *Cyanidium caldarium*, an anomalously pigmented chlorophyte. Arch. Mikrobiol. **32**:270–277.
3. **Auernik KS, Cooper CR, Kelly RM.** 2008. Life in hot acid: pathway analyses in extremely thermoacidophilic archaea. Curr. Opin. Biotechnol. **19**:445–453.
4. **Auernik KS, Kelly RM.** 2010. Physiological versatility of the extremely thermoacidophilic archaeon *Metallosphaera sedula* supported by transcriptomic analysis of heterotrophic, autotrophic, and mixotrophic growth. Appl. Environ. Microbiol. **76**:931–935.
5. **Auernik KS, Maezato Y, Blum PH, Kelly RM.** 2008. The genome sequence of the metal-mobilizing, extremely thermoacidophilic archaeon *Metallosphaera sedula* provides insights into bioleaching-associated metabolism. Appl. Environ. Microbiol. **74**:682–692.
6. **Berg IA, Kockelkorn D, Buckel W, Fuchs G.** 2007. A 3-hydroxypropionate/4-hydroxybutyrate autotrophic carbon dioxide assimilation pathway in Archaea. Science **318**:1782–1786.
7. **Berkner S, Grogan D, Albers SV, Lipps G.** 2007. Small multicopy, non-integrative shuttle vectors based on the plasmid pRN1 for *Sulfolobus acidocaldarius* and *Sulfolobus solfataricus*, model organisms of the (cren-) archaea. Nucleic Acids Res. **35**:e88. doi:10.1093/nar/gkm449.
8. **Bini E, Dikshit V, Dirksen K, Drozda M, Blum P.** 2002. Stability of mRNA in the hyperthermophilic archaeon *Sulfolobus solfataricus.* RNA **8**:1129–1136.
9. **Deigweiher K, Drell TL IV, Prutsch A, Scheidig AJ, Lubben M.** 2004. Expression, isolation, and crystallization of the catalytic domain of CopB, a putative copper transporting ATPase from the thermoacidophilic archaeon *Sulfolobus solfataricus.* J. Bioenerg. Biomembr. **36**:151–159.
10. **Eggert RG, et al.** 2007. Minerals, critical minerals and the U.S. economy. The National Academies Press, Washington, DC.
11. **Ettema TJ, et al.** 2006. Molecular characterization of a conserved archaeal copper resistance (cop) gene cluster and its copper-responsive regulator in *Sulfolobus solfataricus* P2. Microbiology **152**:1969–1979.
12. **Ettema TJ, Huynen MA, de Vos WM, van der Oost J.** 2003. TRASH: a novel metal-binding domain predicted to be involved in heavy-metal sensing, trafficking and resistance. Trends Biochem. Sci. **28**:170–173.
13. **Gonzalez-Guerrero M, Arguello JM.** 2008. Mechanism of Cu+-transporting ATPases: soluble Cu+ chaperones directly transfer Cu+ to transmembrane transport sites. Proc. Natl. Acad. Sci. U. S. A. **105**:5992–5997.
14. **Grogan DW, Gunsalus RP.** 1993. *Sulfolobus acidocaldarius* synthesizes UMP via a standard de novo pathway: results of biochemical-genetic study. J. Bacteriol. **175**:1500–1507.
15. **Hajduch M, Ganapathy A, Stein JW, Thelen JJ.** 2005. A systematic proteomic study of seed filling in soybean. Establishment of high-resolution two-dimensional reference maps, expression profiles, and an interactive proteome database. Plant Physiol. **137**:1397–1419.
16. **Han CJ, Kelly RM.** 1998. Biooxidation capacity of the extremely ther-

moacidophilic archaeon *Metallosphaera sedula* under bioenergetic challenge. Biotechnol. Bioeng. **58**:617–624.
17. **Hoang V, Bini E, Dixit V, Drozda M, Blum P.** 2004. The role of cis-acting sequences governing catabolite repression control of lacS expression in the archaeon *Sulfolobus solfataricus.* Genetics **167**:1563–1572.
18. **Huber G, Spinnler C, Gambacorta A, Stetter K.** 1989. *Metallosphaera sedula* gen. and sp. nov. represents a new genus of aerobic, metal-mobilizing, thermoacidophilic archaebacteria. Syst. Appl. Microbiol. **12**: 38–47.
19. **Huber H, Prangishvili D.** 21 December 2004, posting date. The Sulfolobales. *In* M. Dworkin et al (ed), The prokaryotes: an evolving electronic resource for the microbiological community. Springer-Verlag, New York, NY.
20. **Kappler U, Sly LI, McEwan AG.** 2005. Respiratory gene clusters of *Metallosphaera sedula*-differential expression and transcriptional organization. Microbiology **151**:35–43.
21. **Kondo S, Yamagishi A, Oshima T.** 1991. Positive selection for uracil auxotrophs of the sulfur-dependent thermophilic archaebacterium *Sulfolobus acidocaldarius* by use of 5-fluoroorotic acid. J. Bacteriol. **173**:7698–7700.
22. **Konishi Y, Asai S, Tokushige M, Suzuki T.** 1999. Kinetics of the bioleaching of chalcopyrite concentrate by acidophilic thermophile *Acidianus brierleyi.* Biotechnol. Prog. **15**:681–688.
23. **Liu LJ, You XY, Guo X, Liu SJ, Jiang CY.** 2011. *Metallosphaera cuprina* sp. nov., an acidothermophilic, metal-mobilizing archaeon. Int. J. Syst. Evol. Microbiol. **61**:2395–2400.
24. **Liu LJ, et al.** 2011. Complete genome sequence of *Metallosphaera cuprina*, a metal sulfide-oxidizing archaeon from a hot spring. J. Bacteriol. **193**: 3387–3388.
25. **Long KR, DeYoung JH, Ludington SD.** 1999. Database of significant deposits of gold, silver, copper, lead, and zinc in the United States, p 1–60. U.S. Geological Survey, Reston, VA.
26. **Maezato Y, Dana K, Blum P.** 2011. Engineering thermoacidophilic archaea using linear DNA recombination. Methods Mol. Biol. **765**:435–445.
27. **Maezato Y, et al.** 2011. VapC6, a ribonucleolytic toxin regulates thermophilicity in the crenarchaeote *Sulfolobus solfataricus.* RNA **17**:1381–1392.
28. **Martusewitsch E, Sensen CW, Schleper C.** 2000. High spontaneous mutation rate in the hyperthermophilic archaeon *Sulfolobus solfataricus* is mediated by transposable elements. J. Bacteriol. **182**:2574–2581.
29. **Mikkelsen D, et al.** 2007. Visualisation of pyrite leaching by selected thermophilic archaea: nature of microorganism-ore interactions during bioleaching. Hydrometallurgy **88**:143–153.
30. **Olson GJ, Brierley JA, Brierley CL.** 2003. Bioleaching review part B. Progress in bioleaching: applications of microbial processes by the minerals industries. Appl. Microbiol. Biotechnol. **63**:249–257.
31. **Orell A, Navarro CA, Arancibia R, Mobarec JC, Jerez CA.** 2010. Life in blue: copper resistance mechanisms of bacteria and archaea used in industrial biomining of minerals. Biotechnol. Adv. **28**:839–848.
32. **Ramos-Vera WH, Weiss M, Strittmatter E, Kockelkorn D, Fuchs G.** 2011. Identification of missing genes and enzymes for autotrophic carbon fixation in crenarchaeota. J. Bacteriol. **193**:1201–1211.
33. **Rawlings DE.** 2005. Characteristics and adaptability of iron- and sulfur-oxidizing microorganisms used for the recovery of metals from minerals and their concentrates. Microb. Cell Fact. **4**:13.
34. **Rawlings DE.** 2002. Heavy metal mining using microbes. Annu. Rev. Microbiol. **56**:65–91.
35. **Rawlings DE, Tributsch H, Hansford GS.** 1999. Reasons why "*Leptospirillum*"-like species rather than *Thiobacillus ferrooxidans* are the dominant iron-oxidizing bacteria in many commercial processes for the biooxidation of pyrite and related ores. Microbiology **145**:5–13.
36. **Remonsellez F, Orell A, Jerez CA.** 2006. Copper tolerance of the thermoacidophilic archaeon *Sulfolobus metallicus*: possible role of polyphosphate metabolism. Microbiology **152**:59–66.
37. **Rockabrand D, Austin T, Kaiser R, Blum P.** 1999. Bacterial growth state distinguished by single-cell protein profiling: does chlorination kill coliforms in municipal effluent? Appl. Environ. Microbiol. **65**:4181–4188.
38. **Rohwerder T, Gehrke T, Kinzler K, Sand W.** 2003. Bioleaching review part A. Progress in bioleaching: fundamentals and mechanisms of bacterial metal sulfide oxidation. Appl. Microbiol. Biotechnol. **63**:239–248.
39. **Schelert J, Drozda M, Dixit V, Dillman A, Blum P.** 2006. Regulation of mercury resistance in the crenarchaeote *Sulfolobus solfataricus.* J. Bacteriol. **188**:7141–7150.
40. **Schippers A, Jozsa P-G, Sand W.** 1996. Sulfur chemistry in bacterial leaching of pyrite. Appl. Environ. Microbiol. **62**:3424–3431.
41. **Schippers A, Sand W.** 1999. Bacterial leaching of metal sulfides proceeds by two indirect mechanisms via thiosulfate or via polysulfides and sulfur. Appl. Environ. Microbiol. **65**:319–321.
42. **Sowers KR, Blum PH, DasSharma S.** 2007. Gene transfer in archaea. *In* Reddy C (ed), Methods for general and molecular microbiology, p 800–824. ASM Press, Washington, DC.
43. **Suzuki I.** 2001. Microbial leaching of metals from sulfide minerals. Biotechnol. Adv. **19**:119–132.
44. **USGS.** 2011. Mineral commodity summaries, p 48–49. U.S. Geological Survey, Reston, VA.
45. **Valdes J, Ossandon F, Quatrini R, Dopson M, Holmes DS.** 2011. Draft genome sequence of the extremely acidophilic biomining bacterium *Acidithiobacillus thiooxidans* ATCC 19377 provides insights into the evolution of the *Acidithiobacillus* genus. J. Bacteriol. **193**:7003–7004.
46. **Villafane A, et al.** 2011. CopR of *Sulfolobus solfataricus* represents a novel class of archaeal-specific copper-responsive activators of transcription. Microbiology **157**:2808–2817.
47. **Vollmecke C, Drees SL, Reimann J, Albers SV, Lubben M.** 2012. The ATPases CopA and CopB both contribute to copper resistance of the thermoacidophilic archaeon *Sulfolobus solfataricus.* Microbiology **158**: 1622–1633.
48. **Ward M, et al.** 2002. Evolutionary and revolutionary technologies for mining. National Research Council, Washington, DC.
49. **Worthington P, Hoang V, Perez-Pomares F, Blum P.** 2003. Targeted disruption of the alpha-amylase gene in the hyperthermophilic archaeon *Sulfolobus solfataricus.* J. Bacteriol. **185**:482–488.